European Review for Medical and Pharmacological Sciences 2021; 25: 3967-3980

Ribosomal protein RPS15A augments proliferation of colorectal cancer RKO cells *via* regulation of BIRC3, p38 MAPK and Chk1

B.-S. WAN[1], X.-Y. WANG[2], J. TIANG[3], C. ZHOU[3], J. LIN[4], Z. WANG[3]

[1]Department of General Surgery, Jiading District Central Hospital Affiliated Shanghai University of Medicine & Health Sciences, Shanghai, China
[2]Department of Ultrasound, Renji Hospital, School of Medicine, Shanghai Jiao Tong University, Shanghai, China
[3]Department of Gastrointestinal Surgery, Renji Hospital, School of Medicine, Shanghai Jiao Tong University, Shanghai, China
[4]Department of Ophthalmology, Renji Hospital, School of Medicine, Shanghai Jiao Tong University, Shanghai, China

Abstract. – OBJECTIVE: Ribosomal protein S15A (RPS15A) has been implicated in tumorigenesis, but its role in colorectal cancer (CRC) is not fully studied. The objective of this study was to investigate the role of RPS15A in CRC carcinogenesis.

PATIENTS AND METHODS: RBSP15A expression was detected in 120 colorectal adenocarcinoma biopsies by immunohistological staining, and we examined the association of RSP15A expression with clinicopathological outcomes. We generated RPS15A stable knockdown CRC cell lines using shRNAs and assessed cell proliferation by MTT assays, clonogenicity by colony formation assays, and apoptosis and cell cycle arrest by flow cytometric analyses. A mouse tumor xenograft model was used to confirm the influence of RPS15A expression on CRC *in vivo*.

RESULTS: RPS15A expression was predictive for poor disease-free survival. Knockdown of RPS15A expression significantly inhibited cell proliferation and colony formation and augmented apoptosis in both the RKO and SW620 CRC cell lines. Moreover, RPS15A knockdown arrested RKO cells at the G2/M phase and SW620 cells at the G0/G1 phase. KEGG pathway analysis of 785 genes differentially expressed between wild-type and shRPS15A RKO cells showed enrichment for the pathway in cancer and MAPK signaling pathway KEGG terms. RPS15A knockdown induced apoptosis *via* regulation of BIRC3, p38 MAPK, and Chk1. Consistently, RPS15A knockdown significantly impaired the growth of subcutaneous CRC xenografts in nude mice.

CONCLUSIONS: These results indicate that RPS15A is a novel, potentially oncogenic gene involved in colorectal carcinogenesis. RPS15A knockdown may be an attractive strategy for treating CRC with gene therapy.

Key Words:
Colorectal cancer, RPS15A, SiRNA, Proliferation, Microarray.

Introduction

Colorectal cancer (CRC) is the third most common cancer and the second most frequent cause of cancer-related deaths globally[1-3]. Despite recent implementation of national screening programs and advances in diagnostic and therapeutic approaches, the prognosis for CRC patients whose tumor is not detected until it has been advanced remains poor[4]. Consequently, there is an urgent need to develop novel therapeutic strategies for treating patients with advanced CRC.

Eukaryotes have 80S ribosomes, each consisting of a 40S subunit and a larger 60S subunit. The three-dimensional structures of the RNA molecules within the 40S subunit facilitate the interaction between mRNA codons and tRNA anticodons, whilst those of the 60S subunit catalyzes peptide-bond formation[5]. Ribosomal biogenesis is a highly ordered cellular process for producing ribosomes needed for protein translation and is therefore essential for cell growth and proliferation[6]. Consequently, interference with ribosomal biogenesis can severely delay cell growth and proliferation and impairs larval development in *Drosophila*[7,8]. Several ribosomal proteins (RPs) play pivotal roles in cell transformation and tumorigenesis, presumably arising from their involvement in DNA replication and repair, auto-

Corresponding Author: Zheng Wang, MD; e-mail: wangzh1972@126.com

regulation of RP synthesis and translation, and RNA processing[9]. Overexpression of RPS3a, for example, induces the transformation of NIH3T3 cells and the formation of tumors within nude mice[10]. RPS13, meanwhile, is overexpressed in colon[11], gastric[12], and small cell lung cancer cells[13]; RPS27 is overexpressed in hepatocellular carcinoma[14]; RPS2, RPL7A, RPL23A, RPS14, and RPL19 are overexpressed in malignant prostate cancer cell lines and tissue biopsies[15].

RPS15A is one of ~33 RPs that assemble with an 18S RNA to form the 40S subunit. RPS15A promotes the binding of capped mRNA to the 40S subunit early in translation[16] and interacts with Ca^{2+} and calmodulin to modulate ribosome assembly and translation[17]. RPS15A is also implicated in tumorigenesis. As a gene expression classifier, differential expression of RPS15A in combination with 34 other genes can differentiate between ductal carcinoma *in situ* and invasive breast cancer, implying a potential role in breast cancer progression[18]. Moreover, RPS15A is downregulated in androgen-independent prostate cancer after exposure to 17β estradiol[19]. RPS15A is overexpressed in response to the hepatitis B X antigen and plays a marked role in the development of hepatocellular carcinoma (HCC)[20,21]. *RPS15A* is also a transforming growth factor (TGF) β1-responsive gene and promotes cell proliferation in the A549 lung adenocarcinoma cell line[22], while RPS15A inhibition impairs the proliferation of A549 cells[23]. Consistently, RPS15A is also overexpressed in lung cancer samples[23]. With regards to CRC, RPS15A has been determined to involve in the development of colorectal cancer [24-26].

Patients and Methods

Human CRC Specimens

The present study enrolled 120 patients with colorectal adenocarcinoma who were diagnosed and treated at the Renji Hospital, Shanghai Jiao Tong University School of Medicine, from January to December of 2012. The guidelines of the Chinese Society of Clinical Oncology (2018 version) were strictly followed for CRC diagnosis[27]. A biopsy of diseased tissue was obtained from each patient *via* surgical excision. All samples were obtained with informed consent and used with approval from the Review Board of Renji Hospital. The ages of the patients at diagnosis ranged from 39 to 81 years, with a median age of 69 years. Colorectal samples were classified as a carcinoma, normal carcinoma-adjacent tissue or adenocarcinoma. 5 μm-thick of slides were created from available formalin-fixed paraffin-embedded tissue in accordance with the protocol of the Department of Pathology at Renji Hospital. Data for the age at diagnosis, gender, tumor location, tumor grade, TNM stage, and vital status of patients relative to disease-specific survival at the time of follow-up (median follow-up time = 36 months) were obtained.

Immunohistochemistry

Immunohistochemical staining of RPS15A was conducted on 5 μm-thick formalin-fixed paraffin-embedded samples. First, the slides were heated at 60°C, deparaffinized and hydrated by sequential washes in xylene, graded alcohol, and phosphate-buffered saline (PBS). The RPS15A antigen was retrieved *via* incubation with 0.1 mol/L citrate buffer (pH 6.0) for 30 min at 95°C. The slides were then washed with PBS and incubated with 3% (v/v) H_2O_2 for 10 min at room temperature to quench endogenous peroxidase activity. Following an additional three washes with PBS, the slides were blocked against non-specific epitopes *via* incubation with 10% (w/v) normal goat serum diluted in 1 part (w) bovine serum albumin (BSA, Sangon Biotechnology, Shanghai, China) and 99 parts (v) PBS for 30 min at room temperature. The slides were then incubated with 1 part anti-RPS15A monoclonal antibody (Santa Cruz Biotechnology, Santa Cruz, CA, USA) and 999 parts blocking solution overnight at 4°C. The slides were then washed three times with PBS, incubated in block solution for 10 min at room temperature and labeled with a biotinylated secondary antibody and horseradish peroxidase (HRP)-labeled streptavidin (1:1000 dilution, Santa Cruz Biotechnology) for 1 h at 37°C. Finally, the enzymatic reaction was developed with 3, 3'-diaminobenzidine (DAB, Sangon Biotechnology) for 3 to 5 min, and then the slides were counterstained with hematoxylin (Sigma-Aldrich, St. Louis, MO, USA) for 30 sec and subsequently washed with PBS for 3 to 5 min at room temperature.

The immunostaining of slides with the RPS15A antibody was scored independently by two pathologists. Scoring of RPS15A expression was based on two variables as previously described[28]: the percentage of positively stained tumor cells (0 to <5% positively stained cells = 0, 5-25% positively stained cells = 1 or >50% positively stained cells = 2) and the staining intensity (absent or low staining = 0, moderate staining = 1 or high staining = 2).

The scores for the two variables were then added together to obtain an overall score for each specimen and dichotomized into negative (scores of 0-1) or positive (scores of 2-12) classifications.

Cell Lines

Human CRC cell lines (RKO, SW480, HCT-116, DLD1, HT-29, and SW620) were purchased from the Shanghai Cell Bank (Shanghai, China). All cell lines were maintained in Dulbecco's Modified Eagle's Medium (DMEM; Gibco™, Carlsbad, CA, USA) supplemented with 10% fetal bovine serum (Gibco™) and 0.1% gentamicin sulfate (Sangon Biotechnology) at 37°C in a 5% CO_2 humidified incubator. All experiments were performed using cells grown to >75% confluence.

RNA Extraction and Real-Time Quantitative PCR

RNA was extracted from cells using the TRIzol® reagent (Thermo Fisher Scientific, Waltham, MA, USA) and synthesized into cDNA with the M-MLV reverse transcriptase (Promega, Madison, WI, USA) according to the manufacturer's instructions. Real-time quantitative PCR (qPCR) of cDNA was completed as per the manufacturer's protocol (Promega). The sequences of the GAPDH internal control primers were 5′-TGA CTT CAA CAG CGA CAC CCA-3′ (forward) and 5′-CAC CCT GTT GCT GTA GCC AAA-3′ (reverse). The sequences of RPS15A primers were 5′-CTC CAA AGT CAT CGT CCG GTT-3′ (forward) and 5′-TGA GTT GCA CGT CAA ATC TGG-3′ (reverse). Each qPCR reaction consisted of an initial denaturation step at 95°C for 30 secs, followed by 40 cycles of denaturation at 95°C for 5 s and extension at 60°C for 30 s. The PCR products of RPS15A and GAPDH were 161 and 121 bp, respectively. All samples were tested in triplicate. Relative quantitation of gene expression was calculated using the $2^{-\Delta\Delta CT}$ method.

Construction of Lentiviral Vector and Cell Transfection

The siRNA against the human *RPSI5A* gene (GenBank no. NM_001019) was designed using the full-length *RPSI5A* sequence from GeneChem Co. Ltd (Shanghai, China). The siRNA sequence was 5′-GCA ACT CAA AGA CCT GGA A-3′. For testing the knockdown efficiency, stem-loop-stem oligonucleotides were synthesized and inserted into a pGCSIL-GFP vector (GeneChem Co. Ltd). Lentiviral particles were packaged as previously described[29].

For cell transduction, RKO and SW620 cells (50,000 cells/well) were seeded into 6-well plates and transduced with the recombinant shRPS15A lentivirus or a negative-control (shCtrl) lentivirus at a multiplicity of infection of 20. Cells were incubated at 37°C in a 5% CO_2 humidified incubator. After 72 h, the cells were observed under a fluorescence microscope (MicroPublisher™ 3.3RTV, Olympus Corporation, Tokyo, Japan). After 5 days, the knockdown efficiency was determined by qPCR and Western blot.

MTT Assay

The proliferation of RKO and SW620 CRC cell lines transduced with either a shRPS15A or an empty plasmid was determined with the MTT assay. Transduced RKO and SW620 cells (1,000 cells/well) within the logarithmic phase were seeded in 96-well plates and incubated at 37°C with 5% CO_2 for 5 consecutive days. Next, 10 μL of 5 mg/mL MTT (3-(4,5-dimethylthiazol-2-yl)-2,5-diphenyltetrazolium bromide, DingGuoBio, Beijing, China) was added to each well and incubated for 4 h at each termination of culture. Afterward, the supernatant was discarded, whereupon 100 μL of dimethylsulfoxide (DMSO, Sinopharm, Shanghai, China) was added to each well and incubated in an air bath shaker at 37°C for 10 min. The A490 nm was measured with an Elx-800 microplate reader (Biotek, Winooski, VT, USA).

Colony Formation Assay

The effect of RPS15A knockdown on subsequent colony formation was determined in parallel with a negative control. Transfected RKO and SW620 cells (1,000 cells/well) were seeded in 6-well plates and incubated for 10 days to form colonies. The medium was renewed every 2 days. Cells were washed with PBS (pH 7.2) and fixed with 4% paraformaldehyde (Sangon Biotechnology) for 30-60 min. The fixed cells were washed with PBS and then stained with 100 μl of Giemsa staining solution (Chemicon International, Temecula, CA, USA) for 20 min at room temperature. The total number of colonies consisting of >50 cells was counted using light microscopy.

Flow Cytometric Analyses of Cell Cycle Stage and Apoptosis

The effect of RPS15A knockdown on cell cycle progression and apoptosis was determined by flow cytometry (FCM). Four days post lentiviral infection, RKO and SW620 cells were reseeded in 6-cm dishes at a density of 1×10^6 cells/dish. Cells were harvested when the coverage rate of cells was >70% and subsequently fixed with 70% ice-cold ethanol

for 1 h at 4°C. The cells were then washed with PBS (pH 7.2), and then DNA was stained by incubation with 1.5 mL PBS containing 50 µg/mL propidium iodide (PI, Sigma-Aldrich) and 100 µg/mL RNase A (Thermo Fisher Scientific) in the dark for 30 min at room temperature. The suspension was filtered through a 45-µm mesh prior to FCM analysis using a FACS Calibur FCM instrument (BD Biosciences, San Diego, CA, USA) to determine the cell cycle phase. All experiments were performed in triplicate.

To identify cells undergoing apoptosis, RKO and SW620 cells were cultured in 6-well plates. Five days post lentiviral infection, transduced cell lines were collected and washed with ice-cold PBS (pH 7.2). Then, the cell concentrations were adjusted to 1×10^6/mL with 1× staining buffer. 100 µL of suspended cells were stained with 5 µL of Annexin V-APC (eBioscience, Cat no.88-8007, San Diego, CA, USA) and incubated in the dark at room temperature for 10-15 min. Cells were analyzed by FCM within 1 h. All experiments were performed in triplicate.

RNA Isolation and Microarray Analysis

The expression status of 20,000 genes in individual microarrays (GeneChip Primeview Human Gene Expression Array; Cat No. 901838, Affymetrix, Santa Clara, CA, USA) was determined for RKO cells transfected with either the shRPS15A or shCtrl lentiviruses. Initially, RNA was isolated from RKO cells 72 h post transfection using the Trizol reagent (Thermo Fisher Scientific). For gene expression profiling, individual microarrays were used for each sample. Briefly, 0.5 µg of RNA was used to synthesize cDNA. Biotin-labeled amplified RNA was synthesized from a double-stranded cDNA using the GeneChip® 3′ IVT labeling kit (Affymetrix). The wash and staining protocols were performed with the GeneChip® Hybridization Wash and Stain Kit (Affymetrix) using a GeneChip® Fluidics Station 450 (Affymetrix) according to the manufacturer's instructions. Finally, the probe arrays were scanned directly using a GeneChip® Scanner 3000 (Affymetrix) post hybridization.

Microarray Data Normalization and Analysis

The GeneSpring v11 software (Agilent Technologies, Santa Clara, CA, USA) was used to analyze microarray data. Initially, data were normalized using the GeneSpring software according to the manufacturer's instructions. The normalized data were used to generate lists of genes differentially expressed by at least ±1.5-fold and also deemed statistically significant ($p \leq 0.05$) according to the Student's *t*-test relative to the negative control. A list of transcripts that were differentially expressed as a function of treatment was generated, which was clustered hierarchically using the GeneSpring software based on the manufacturer's instructions. Enriched pathways were identified using the KEGG and BIOCARTA software. Finally, gene sets with meaningful and significantly different expressions were utilized to identify molecular functions using qPCR and Western blot. The primers used for qPCR are listed in Table I.

Table I. The qPCR primers used in the present study.

GenBank no.	Gene	Primers	Fragment size (bp)
NM_002392	MDM2	Forward:GAATCATCGGACTCAGGTACATC Reverse:TCTGTCTCACTAATTGCTCTCCT	167
NM_001010935	RAP1A	Forward:CGTGAGTACAAGCTAGTGGTCC Reverse:CCAGGATTTCGAGCATACACTG	166
NM_032991	CASP3	Forward:GTTCATCCAGTCGCTTTGTGC Reverse:ATTCTGTTGCCACCTTTCGG	98
NM_001195054	DDIT3	Forward:CTTCTCTGGCTTGGCTGACTGA Reverse:TGACTGGAATCTGGAGAGTGAGG	88
NM_002881	RALB	Forward:TCATCAGGAAAGGAGCACT Reverse:GAGGGGATACAGGATTGTT	189
NM_001165	BIRC3	Forward:TTTCCGTGGCTCTTATTCAAACT Reverse:GCACAGTGGTAGGAACTTCTCAT	96
NM_002228	JUN	Forward:CGCCAAGAACTCGGACCTC Reverse:CCTCCTGCTCATCTGTCACG	164
NM_001143820	ETS1	Forward:CCTCACCGCCAACTCTGT Reverse:TCTCACCTGACATCCTACCG	232
NM_005252	FOS	Forward:GAAGCCAAGACTGAGCCG Reverse:GCGGGTGAGTGGTAGTAAGAG	231
NM_006908	RAC1	Forward:ATGTCCGTGCAAAGTGGTATC Reverse:CTCGGATCGCTTCGTCAAACA	249

Western Blot

The expression of genes related to apoptosis was determined at the protein level by targeted immunostaining with specific antibodies. 48 h post lentiviral infection, cells were lysed using ice-cold lysis buffer (100 mM Tris, pH 6.8, 2% b-mercaptoethanol, 20% glycerol, and 4% SDS). The lysates were centrifuged for 10 min at 12,000 g and 4°C, whereupon the supernatants were collected, and protein concentrations determined using a BCA Protein Assay Kit (HyClone-Pierce, Logan, UT, USA). Equal amounts (20 μg) of protein samples of each treatment were separated by 10% sodium dodecyl sulphate-polyacrylamide gel electrophoresis (SDS-PAGE) according to Laemmli's method[30] and transferred to polyvinylidene difluoride (PVDF) membranes. Membranes were incubated in TBST (25 mM Tris, pH 7.4, 150 mM NaCl and 0.1% Tween-20) containing 5% skimmed milk for 1 h at room temperature. Next, the membranes were incubated overnight at 4°C with the following primary antibodies: mouse monoclonal anti-Flag® M2 (1:1,000 dilution, Cat no. F1804, Sigma-Aldrich), rabbit polyclonal anti-FOS (1:200 dilution, Cat no. Ab7963, Abcam, Cambridge, MA, USA), rabbit monoclonal anti-Casp3 (1:1,000 dilution), rabbit anti-cleaved Casp3 (1:5,000 dilution, Cat no. #9664, Cell Signaling Technology, Beverly, MA, USA), mouse monoclonal anti-RAP1A (1:1,000 dilution, Cat no. Ab55741, Abcam), rabbit polyclonal anti-RAC1 (1:500 dilution, Cat no. Ab97568, Abcam), rabbit monoclonal anti-BIRC3 (1:1,000 dilution, Cat no. Ab32059, Abcam), mouse monoclonal anti-RALB (1:4,000 dilution, Cat no. Ab156799, Abcam) and mouse monoclonal anti-GAPDH (1:2,000 dilution, Cat no. sc-32233, Santa Cruz Biotechnology). Finally, Western blots were incubated with a goat anti-mouse (1:5,000 dilution, Cat no. sc-2005, Santa Cruz Biotechnology) or goat anti-rabbit horseradish peroxidase (1:5,000 dilution, Cat no. sc-2004, Santa Cruz Biotechnology) secondary antibody for 1 h at 37°C. Signals were detected with an ECL-PLUS kit (Cat no. RPN2132, Amersham, Arlington Heights, OH, USA) according to the manufacturer's instructions. GAPDH was used as the internal control.

Stress and Apoptosis Signaling Antibody Array

Cell lysates were prepared from RKO cells transduced with either the shRPS15A or shCtrl lentiviruses. Stress and apoptosis signaling molecules were detected using a PathScan® stress and apoptosis signaling array kit (Cell Signaling Technology, #12856) according to the manufacturer's instructions.

Mouse Tumor Xenograft Model

Tumor engraftment in nude mice was done as described previously[31]. Briefly, two groups of 4-week old nude mice were subcutaneously injected at the right axilla with cells successfully transduced with either the shRPS15A or the control lentivirus. The average tumor size was determined by physical measurement of the excised tumor at the time of mouse sacrifice. With the exception of mice with large tumors, animals were sacrificed 4 weeks after injection. All procedures were performed in accordance with standard guidelines as described in the Guide for the Care and Use of Laboratory Animals (US National Institutes of Health 85-23, revised 1996). All animal protocols were agreed with the local Institutional Animal Care and Use Committee of Shanghai Jiao Tong University.

Statistical Analysis

All categorical data are expressed as a frequency. The associations between RPS15A expression in human samples and clinical variables were analyzed using the Fisher's exact test and ROC curve analysis. The association between tumor expression of RPS15A and patient disease-specific survival was fitted with Kaplan-Meier survival curves and assessed with a log-rank test. A Cox proportional hazards model was fitted for multivariable analysis. Numerical data are expressed as the mean ± SD, for which the Student's *t*-test was used to determine significance. All statistical analyses were conducted using the SPSS v.16 software (SPSS, Inc., Chicago, USA). A *p*-value less than 0.05 was considered statistically significant.

Results

RPS15A Expression in Human Colorectal Carcinomas

To explore potential associations between RPS15A expression and clinicopathological outcomes of human colorectal carcinoma diagnoses, we first used immunohistochemical staining to assess RPS15A expression in tumors resected from 120 patients diagnosed with colorectal adenocarcinoma. Of the 120 cancer specimens, 104

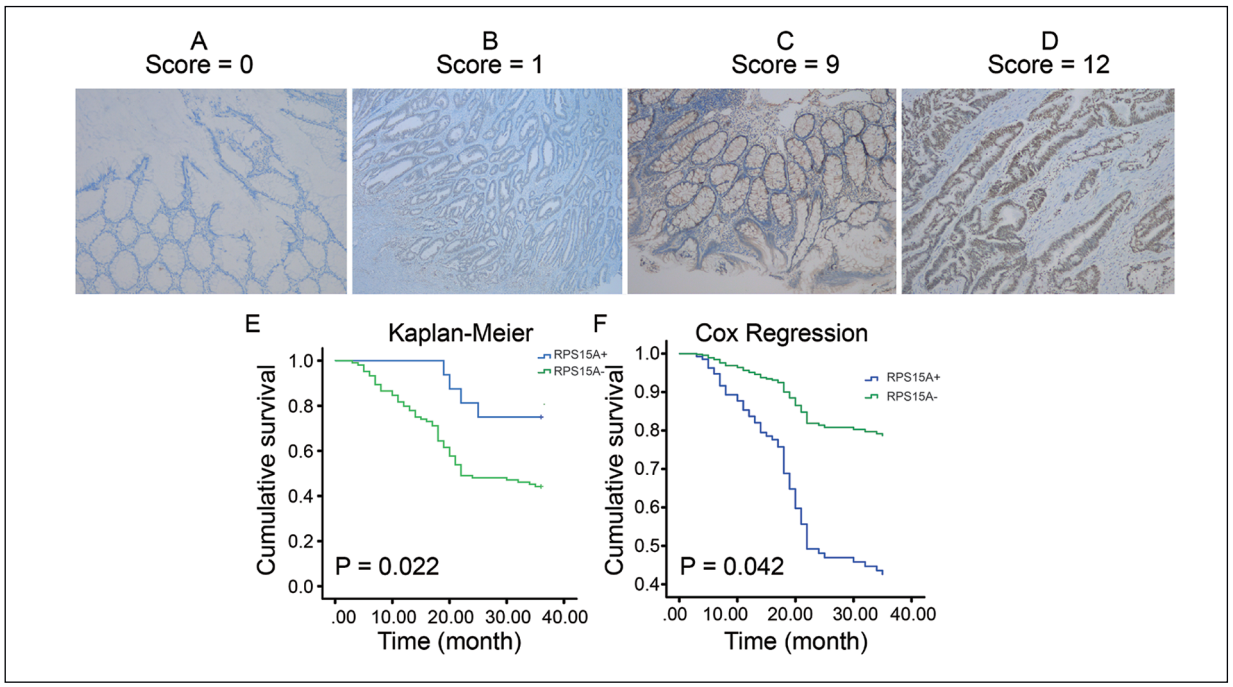

Figure 1. RPS15A expression in 120 human colorectal carcinoma biopsies. **A-D**, Representative RPS15A immunohistochemical staining in human colorectal tumor samples (x100 magnification). Negative (A score = 0; B score = 1) and positive scores (C score = 9; D score = 12). (**E**) Kaplan-Meier and (**F**) Cox regression models of disease-specific mortality for patients whose colorectal tumors expressed positive and negative levels of RPS15A. The log-rank test (two-sided) was used to compare differences between groups.

(86.7%) were positive for RPS15A expression (Figure 1A-D). The clinicopathological data for these 120 patients is presented in Table II. The median age at diagnosis was 61 years (ranging

Table II. Univariate analysis of clinicopathological variables and RPS15A expression.

Variable	Total	RPS15A expression*		χ^2	$p^\dagger$
		Negative (%)	Positive (%)		
Age				0.163	0.687
≤ 60	47	7 (14.9)	40 (85.1)		
> 60	73	9 (12.3)	64 (87.7)		
Gender				1.816	0.197
Male	71	7 (9.9)	64 (90.1)		
Female	49	9 (18.4)	40 (81.6)		
Location				1.662	0.197
Rectum	84	9 (10.7)	75 (89.3)		
Colon	36	7 (19.4)	29 (80.6)		
Grade				11.209	0.004
High	24	10 (41.7)	14 (58.3)		
Mediate	42	5 (11.9)	37 (88.1)		
Low	54	1 (1.9)	53 (98.1)		
TNM stage				5.140	0.023
0-I	32	8 (25.0)	24 (75.0)		
II-III	88	8 (9.1)	80 (90.9)		

*RPS15A expression was dichotomized into negative (overall score 0-1) and positive (2-12) groups for analysis. Overall score was obtained by adding the assigned values for RPS15A staining intensity (range 0-2) and percentage of tumor cells staining for RPS15A (range 0-2). †Fisher exact test (two-sided).

from 39 to 81 years). Positive tumor RPS15A expression was significantly associated with advanced tumor stage (p=0.023) and high tumor grade (p=0.004). There was no association between tumor RPS15A expression and age at diagnosis, gender nor tumor location.

Next, the association between RPS15A expression within tumors and patient survival outcomes was evaluated. The median survival for patients positive and negative for tumor RPS15A expression was 22 and 32 months, respectively (p=0.022; Figure 1E). Furthermore, Kaplan-Meier models showed a greater cumulative mortality from CRC for patients with RPS15A-positive tumors. Additionally, positive tumor RPS15A expression remained significantly associated with patient survival and tumor location, stage and grade after Cox regression analysis (Table III). Patients with medium (HR=6.70, 95% CI=1.86 to 24.18) or high-grade tumors (HR=3.43, 95% CI=1.10 to 10.72; p=0.011) had increased hazards of mortality relative to those with low-grade tumors. High RPS15A expression was significantly associated with poor disease-free survival (HR=3.55, 95% CI=1.05 to 12.06; p=0.042; Figure 1F). Patients with colon cancer had lower hazards of related mortality (HR=0.27, 95% CI=0.15 to 0.49; p<0.001) than those with rectal cancer.

Table III. Multivariable analysis of the associations between clinicopathological variables and disease-specific survival in CRC patients*.

Variable	HR (95% CI)	$p^{\dagger}$
Gender		0.113
Female	1.00 (baseline)	
Male	0.58 (0.30-1.14)	
Location		< 0.001
Rectum	1.00 (baseline)	
Colon	0.27 (0.15-0.49)	
Grade		0.011
Low	1.00 (baseline)	
Medium	6.70 (1.86-24.18)	
High	3.43 (1.10-10.72)	
TNM Stage		0.859
0-I	1.00 (baseline)	
II-III	0.92 (0.37-2.28)	
RPS15A expression		0.042
Positive	1.00 (baseline)	
Negative	3.55 (1.05-12.06)	

*HR = hazard ratio of death from colorectal cancer; CI = confidence interval. †Two-sided, from Cox proportional hazards model (verified to conform to proportional hazards assumptions).

RPS15A mRNA Expression in Six CRC Cell Lines

RPS15A mRNA expression in the RKO, SW480, HCT116, DLD1, HT-29, and SW620 CRC cell lines were determined by RT-PCR. The RKO, HT-29, and SW620 cell lines showed the highest expression of *RPS15A* (Figure 2A).

Decreased Expression of RPS15A in RKO and SW620 CRC Cells Transduced with shRPS15A

To elucidate the function of RPS15A in CRC, RPS15A expression was knocked down in RKO and SW620 cells by transduction with a lentivirus

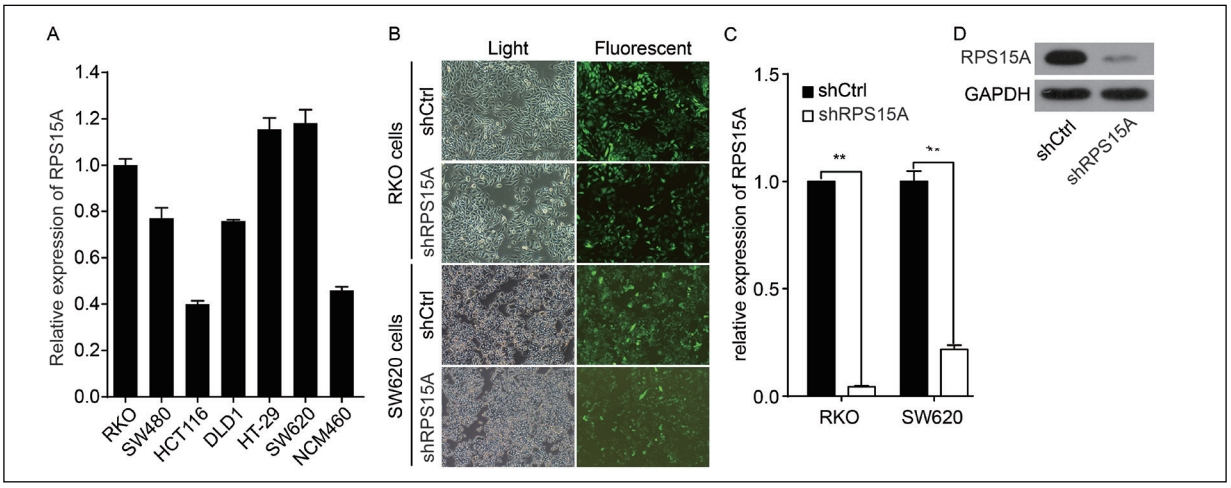

Figure 2. *RPS15A* mRNA levels in six CRC cell lines. **A**, Expression of *RPS15A* mRNA was measured by RT-PCR in the indicated cell lines. *GAPDH* mRNA expression was used as an internal control. **B**, Representative micrographs of GFP expression in control and shRPS15A groups (×200 magnification). **C**, RT-qPCR analysis of RPS15A knockdown efficacy in RKO and SW620 cells transfected with shRPS15A. **p<0.01 compared to control cells. **D**, Assessment of RPS15A knockdown efficacy by Western blot in RKO cells transduced with shRPS15A.

delivering an siRNA payload specifically targeting human RPS15A (shRPS15A). The efficacy of this transduction was >70% (Figures 2B). To evaluate the knockdown efficacy, we isolated mRNA and protein from RKO and SW620 cells transduced with either a shRPS15A or a control payload and subsequently determined the expression of RPS15A mRNA and protein by RT-qPCR and Western blot, respectively. As shown in Figure 2C, the levels of *RPS15A* mRNA were markedly lower in the shRPS15A group than in the shCtrl group. The results suggested that siRNA knockdown was specific to the target gene and that RPS15A loss-of-function was not possibly caused by an off-target effect. Consistently, RPS15A protein expression was reduced by RPS15A knockdown (Figure 2D). These results suggested that shRPS15A could significantly down-regulate RPS15A expression in RKO and SW620 CRC cells.

RPS15A Knockdown in RKO Cells Inhibits Cell Proliferation

To examine the effect of RPS15A expression on cell growth, RKO and SW620 cell lines transduced with either a shRPS15A or control lentiviruses were seeded in 96-well plates and analyzed by Cellomics every day for 5 days. As illustrated in Figures 3A and 3D and confirmed by quantification in Figures 3B and 3E, cells transfected with the control lentivirus greatly expanded over the 5 days of observation, while the number of shRPS15A-transfected cells remained static. The results of the study showed that RPS15A knockdown significantly inhibited the proliferation of RKO and SW620 cells. Furthermore, determination of cell proliferation by MTT assays showed that control cells proliferated almost four-fold from their original number within 5 days, whilst proliferation of RPS15A-knockdown cells was markedly lower by comparison ($p<0.01$, Figures 3C and 3F). Therefore, the proliferation of RKO and SW620 cells was significantly impeded by RPS15A knockdown.

Knockdown of RPS15A Restricts Formation of RKO Colonies

The influence of RPS15A knockdown on the abilities of RKO and SW620 cells to form colo-

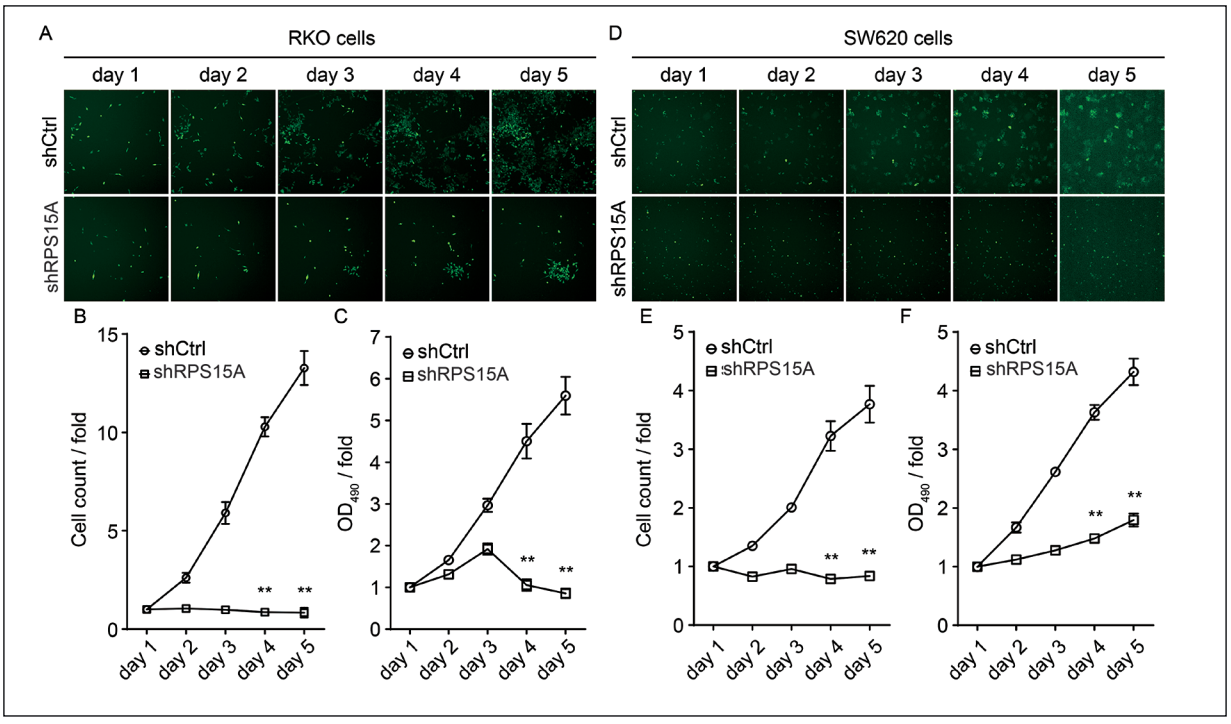

Figure 3. Influence of RPS15A knockdown on RKO and SW620 cell growth. **A** and **D**, Cells were infected with either a control or shRPS15A lentivirus (×200 magnification). High content cell imaging was applied every day as indicated to acquire raw images (unprocessed by software algorithm) of cell growth. **B** and **E**, Cells were seeded in 96-well plates and infected with control or shRPS15A lentivirus, and cell growth was assayed every day for 5 days. $p<0.05$ (control vs. shRPS15A). Cell growth rate was monitored on the 1st, 2nd, 3rd, 4th, and 5th days. $p<0.05$ (control *vs.* shRPS15A). **C** and **F**, Growth curves of control and shRPS15A groups as measured by MTT assays. $^{**}p<0.01$ compared to control cells.

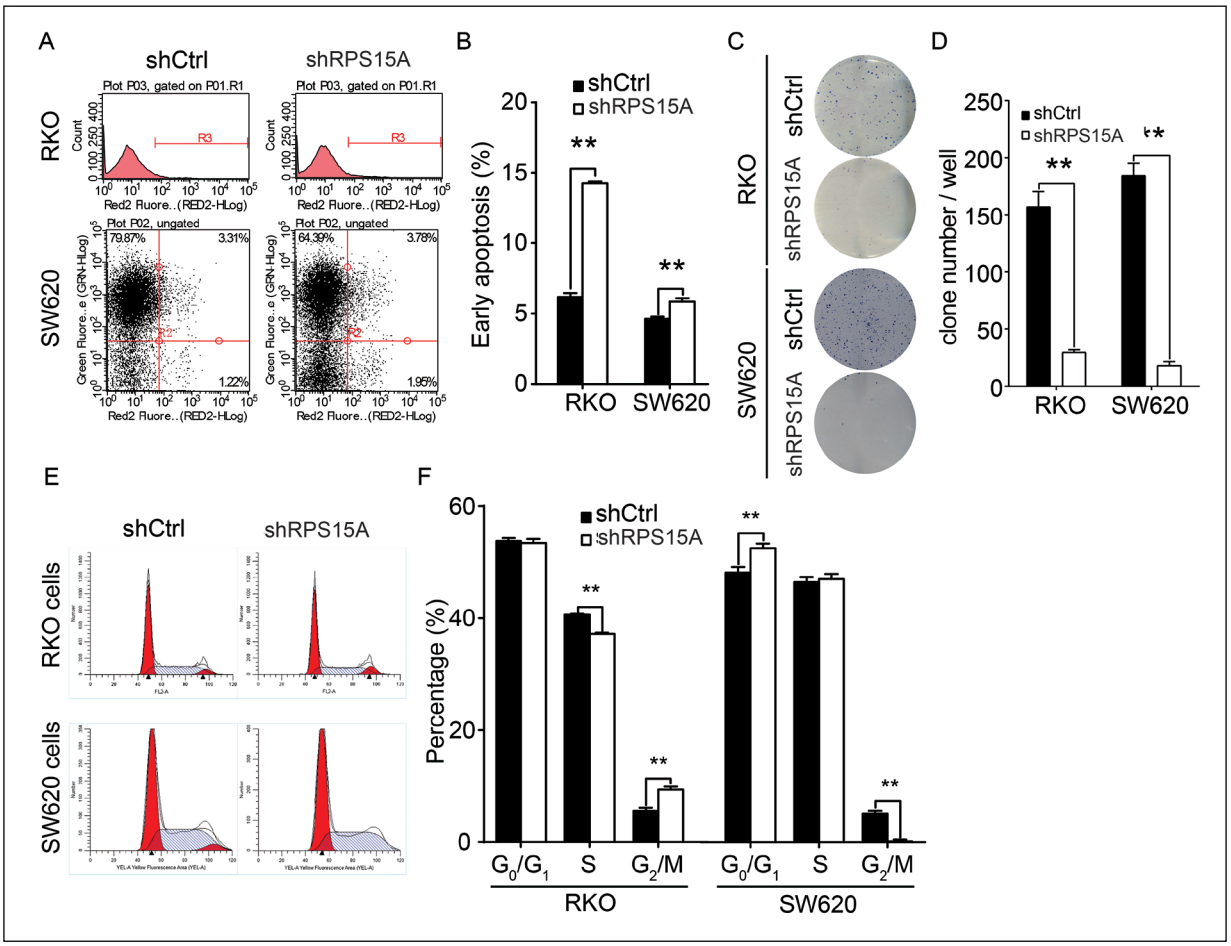

Figure 4. Decreased RPS15A expression impedes colony formation of CRC cells. **A** and **B**, Representative micrographs of colony number in control and shRPS15A groups. **C** and **D**, Colony formation in RKO and SW620 cells transduced with either a shRPS15A or control payload (×40 magnification). $^{**}p<0.01$ compared to control cells. **E**, RPS15A knockdown increases apoptosis in the CRC cells. Representative micrographs of SW620 cells are shown. Each group is shown in triplicates. **F**, Proportions of RKO and SW620 cells transduced with either a shRPS15A or control payload undergoing apoptosis. Note the significant increase in apoptosis in the shRPS15A cultures compared to control cells ($^{**}p < 0.01$).

nies was determined. The impairment of colony formation by RPS15A knockdown was apparent, as presented in Figures 4A and 4B. Consistently, the total number of colonies produced from RPS15A-knockdown cells was significantly lower than those formed by control cells ($p<0.01$; Figure 4C and 4D).

Knockdown of RPS15A in RKO Cells Leads to Cell Cycle Arrest

To determine the contribution of cell cycle arrest to the observed growth inhibition, we determined the cell cycle distributions of RKO and SW620 cells using FCM. The knockdown of RPS15A decreased the number of cells in the G_0/G_1 and S phases and arrested RKO cells in the G_2/M phase, where the proportion of cells within this phase was over 1.5-fold greater than control cells. However, knockdown of RPS15A in SW620 cells arrested their progression in the G_0/G_1 phase, with fewer cells in the G_2/M phase (Figure 4E, F). Collectively, these results suggest that RPS15A knockdown is able to arrest the cell cycle progression of RKO and SW620 cells, leading to decreased cell growth.

Knockdown of RPS15A in RKO and SW620 Cell Lines Increases Apoptosis

To determine whether RPS15A knockdown induced apoptosis in CRC cell lines, we determined the number of cells undergoing apoptosis by Annexin V staining and FCM (Figures 4E). As shown in Figure 4F, cell apoptosis was significantly greater in RPS15A knockdown cells

compared to control cells ($p<0.01$). These results indicate that RPS15A expression is a determinant of cell apoptosis in RKO and SW620 cells.

RPS15A Knockdown in RKO Cells Significantly Alters Gene Expression

Twenty-thousand genes were microarrayed to determine the influence of RPS15A knockdown on downstream gene expression. Relative to the shCtrl RKO cells, 785 genes were differentially expressed in RPS15A-knockdown RKO cells (± 1.5-fold change; $p<0.05$), 631 of which were up-regulated whilst the remaining 154 were down-regulated genes (Figure 5A). KEGG pathway enrichment analysis of these 785 differentially expressed genes identified several pathways de-regulated in cancer, including the pathway in cancer, MAPK signaling pathway, P53 signaling pathway, and cell cycle KEGG terms (Figure 5B).

Knockdown of RPS15A Promotes Cell Apoptosis Via Regulation of BIRC3, p38 MAPK, and Chk1

To understand the molecular mechanisms underlying RPS15A-mediated RKO cell growth, qPCR was used to detect the expression levels mRNA transcripts of apoptosis molecules in RKO cells following RPS15A knockdown (Figure 5C). The expression levels of the *MDM2*, *RAP1A*, *CASP3*, *DDIT3*, *RALB*, *BIRC3*, *JUN*,

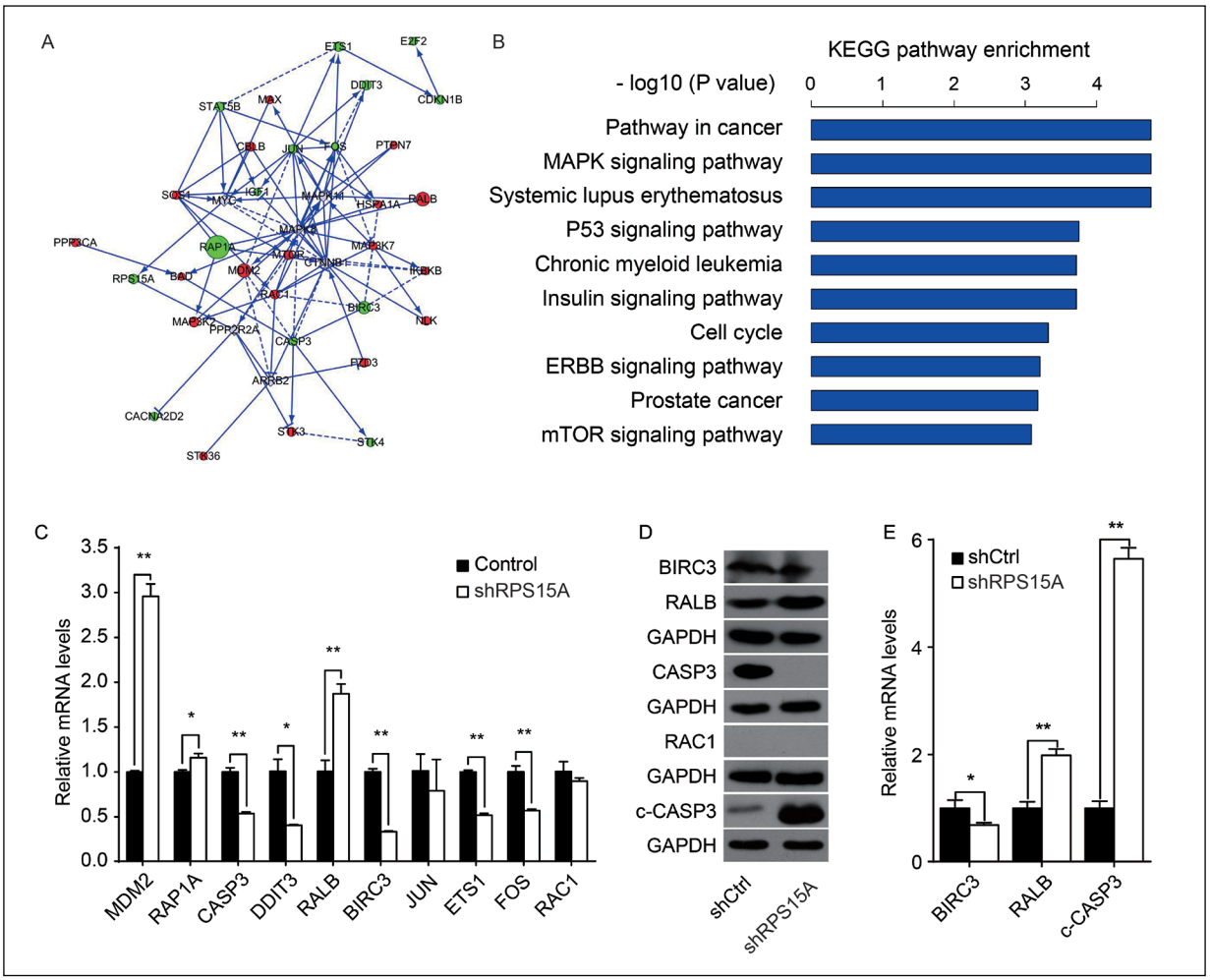

Figure 5. Knockdown of RPS15A in RKO cells significantly alters gene expression. **A**, Hierarchical clustering of differentially expressed transcripts. **B**, KEGG pathway enrichment of differentially expressed genes in RKO cells transduced with the shRPS15A lentivirus compared to control cells. **C,** Quantitative PCR and **D,** western blot confirmation of mRNA expression of MDM2, RAP1A, CAP3, DDIT3, RALB, BIRC3, JUN, ETS1, FOS and RAC1 in RKO cells transfected with either a control or shRPS15A lentivirus. **E,** Quantitative PCR of mRNA expression of BIRC3, RALB and c-CASP3 in RKO cells transfected with control lentivirus and shRPS15A lentivirus. Data represented as the mean ± SD of arbitrary densitometric values of targets/GAPDH. * $p < 0.05$.

ETS1, *FOS,* and *RAC1* mRNAs were downregulated following RPS15A knockdown. These results suggest that RPS15A knockdown could significantly inhibit the growth of RKO cells by blocking the activities of these genes. Furthermore, Western blot showed that knockdown of RPS15A led to a marked decrease in BIRC3 and CASP3 expression, whereas the expression of cleaved CASP3 was markedly increased (Figures 5D and 5E). The results from the PathScan® stress and apoptosis signaling array showed that the knockdown of RPS15A increased expression of phosphorylated p38 MAPK (Thr180/Tyr182) but decreased expression of phosphorylated Chk1 (Ser345). These results suggest that knockdown of RPS15A in RKO cells caused cell apoptosis *via* regulation of BIRC3, phospho-p38 MAPK, and phospho-Chk1.

RPS15A Knockdown Inhibits Tumor Growth In Vivo

Finally, to determine the potential of shRPS15A as a therapeutic tool for treating CRC, nude mice were subcutaneously injected with cells successfully transduced with either the shRPS15A or control lentiviruses. One week following injection, tumors from mice injected RPS15A knockdown cells were smaller compared to the tumors from mice that received control cells (Figures 6A and 6B). Furthermore, the volumes of RPS15A knockdown tumors increased very little up to 10 days after the injection (Figure 6C). This result suggests that shRPS15A suppressed RPS15A expression *in vivo*. These data indicate that targeting RPS15A with shRPS15A lentivirus could have an inhibitory effect on CRC growth *in vivo*.

Discussion

Several lines of evidence suggest a potential role of RPS15A in tumor biology, particularly in tumor development and progression. Overexpression of RPS15A, for example, is induced by hepatitis B X antigen, thereby contributing to

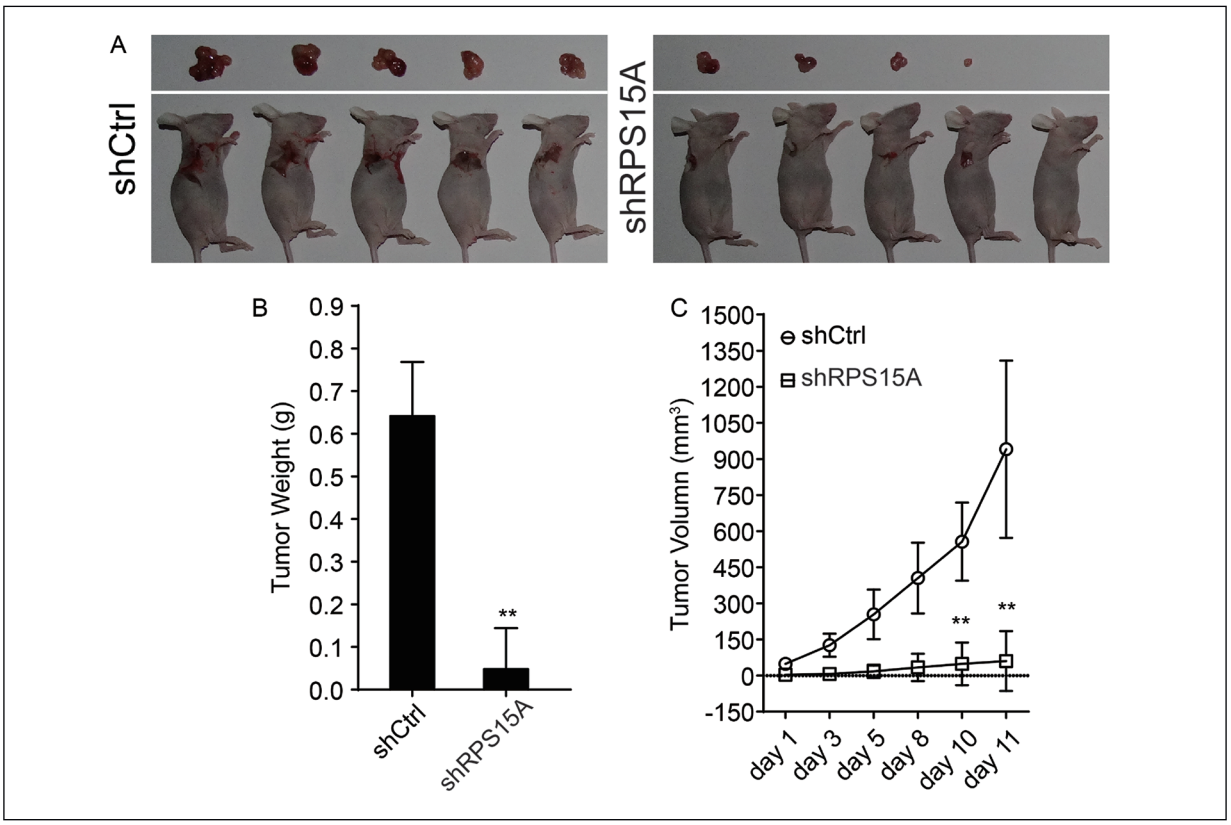

Figure 6. RPS15A knockdown impairs the growth of subcutaneous RKO cell xenografts in nude mice. **A** and **B**, The tumor size of the shRPS15A-transduced cell group was significantly decreased compared to that of the control-transfected cell group. **C**, Tumor growth curves showed a significant growth tendency in the control-transfected cell group, while tumor growth in the shRPS15A-transfected cell group was clearly inhibited ($p<0.01$).

hepatocarcinogenesis[20], while downregulation of RPS15A conversely inhibits hepatic cancer cell growth[21]. Furthermore, RPS15A is a TGF-b-responsive gene in the A549 lung cancer cell line[22] and augments cell proliferation[23]. Therefore, the current study sought to analyze RPS15A expression within biopsies excised from colorectal carcinoma patients and to investigate its association with clinicopathological outcomes. The present study also investigated the influence of RPS15A knockdown in CRC cell lines on their subsequent proliferation, cell cycle distribution, and downstream signaling pathways.

First, we verified by immunohistochemistry that RPS15A was upregulated in human colorectal tumor tissue, suggesting that RPS15A expression contributes toward tumor progression. The present data is consistent with the study by Zhao et al[23], who reported that RPS15A was overexpressed in lung cancer tissues. Of potential clinical importance, we showed that RPS15A expression is significantly associated with poor patient outcomes in CRC, dependent on tumor location and grade but independent of TNM stage.

To give an initial insight into the molecular function of RPS15A in CRC, we measured RPS15A in six CRC cell lines and found high levels of expression in the RKO and SW620 lines. We then evaluated the function of RPS15A in cell growth *via* RPS15A knockdown models created by transduction of RKO and SW620 lines with a lentivirus carrying a shRPS15A payload. This knockdown of RPS15A expression impeded cell proliferation and colony formation and augmented apoptosis in both cell lines. Moreover, knockdown RKO and SW620 cells were frequently arrested at the G_2/M and G_0/G_1 phases, respectively, in contrast to previous studies. For example, although RPS15A silencing inhibited cell proliferation and impaired colony formation in HCC[21] and lung cancer cells[23], these two cell types were arrested at the G_0/G_1 phase. This is best explained by the arrest at different phases in the RPS15A knockdown being dependent upon the genetic background of the lineage of the cells in which it occurs.

To reveal the molecular mechanisms underlying RPS15A-mediated RKO cell proliferation, we determined the expression profiles of 20,000 genes following RPS15A knockdown in RKO cells. Knockdown of RPS15A in RKO cells resulted in the deregulation of 785 genes, 631 of which were upregulated, while the remaining 154 were downregulated. KEGG pathway enrichment of these 785 differentially expressed genes identified them as being involved in the pathway in cancer, MAPK signaling pathway, p53 signaling pathway, and cell cycle KEGG terms. Integration of expression data at the mRNA and protein levels demonstrated that RPS15A knockdown downregulated BIRC3 and phospho-Chk1 but upregulated phospho-p38 MAPK. BIRC3 is an inhibitor of apoptosis (IAP)[32] that serves key oncogenic roles in many cancers, including CRC[33,34]. BIRC3, for example, protects endometrial cancer cells from apoptosis mediated by AP1-59 (an AKT inhibitor)[35]. Conversely, BIRC3 knockdown promotes apoptosis in 1889c squamous thymus cancer cells[36]. Caspase-dependent apoptosis occurs *via* stimulation of the extrinsic or intrinsic pathways, resulting in the downstream activation of effector caspases, including procaspase 3 in some cell lines, and eventually initiating apoptosis[37]. Researches[37-39] have demonstrated that the activation of caspase 3 (CASP3) induces apoptosis in the RKO CRC cell line. However, we found that CASP3 expression decreased and that the expression of cleaved CASP3 was markedly increased in RKO cells with silenced RPS15A. Perhaps then the knockdown of RPS15A induces apoptosis in CRC cells *via* the downregulation of BIRC3 and not by CASP3 activation.

Blocking repair pathways of DNA damage can lead to genomic instability, a hallmark of cancer[40]. Some studies have shown that the ATR-Chk1 pathway, one of the master regulators of the DNA damage-induced checkpoint response[40,41], is required to arrest cells in the G_2 phase[42-44]. Moreover, p38 MAPK arrests cells exposed to ultraviolet radiation at the G_2/M checkpoint[40,45]. Our analysis of the cell cycle distribution showed that RPS15A knockdown arrested cells at the G_2/M stage. Furthermore, the present study demonstrated that RPS15A silencing attenuates the activation of Chk1 *via* an increase in p38 MAPK activity. Thus, the mechanisms of RPS15A knockdown restricting CRC cell growth may occur, in part, *via* the blockade of Chk1 and activation of BIRC3 and p38 MAPK.

We also demonstrated that RPS15A knockdown markedly impaired subcutaneous RKO xenograft growth in nude mice. These results suggest that RPS15A overexpression may be essential for maintaining proliferation and survival, and inhibiting the onset of apoptosis in CRC cells. The present study further validates the an-

ti-apoptosis mechanism of RPS15A in RKO and other CRC cell lines.

Conclusions

We identified that RPS15A is overexpressed in CRC and modulates cell growth. The mechanisms of RPS15A knockdown in inhibiting CRC cell proliferation and cell cycle progression might be partially through the blockade of Chk1 and activation of BIRC3 and p38MAKP. This study may provide a preliminary insight toward the use of a RPS15A-targeted gene therapy for treating CRC.

Conflict of Interest

The Authors declare that they have no conflict of interests.

Funding

This project was supported by Jiading District Science and Technology Commission (JDKW-2017-W03).

Acknowledgements

We would like to thank TopEdit (www.topeditsci.com) for English language editing of this manuscript.

Authors' Contribution

WB performed all experiments and analyses. WX, TJ, ZC, and LJ helped with experiments and figure preparation. WZ designed the project and drafted and revised the manuscript.

References

1) Cunningham D, Atkin W, Lenz HJ, Lynch HT, Minsky B, Nordlinger B, Starling N. Colorectal cancer. Lancet 2010; 375: 1030-1047.
2) Lima JP, de Souza FH, de Andrade DA, Carvalheira JB, dos Santos LV. Independent radiologic review in metastatic colorectal cancer: systematic review and meta-analysis. Radiology 2012; 263: 86-95.
3) Siegel RL, Miller KD, Jemal A. Cancer statistics, 2015. CA Cancer J Clin 2015; 65: 5-29.
4) Qian WF, Guan WX, Gao Y, Tan JF, Qiao ZM, Huang H, Xia CL. Inhibition of STAT3 by RNA interference suppresses angiogenesis in colorectal carcinoma. Braz J Med Biol Res 2011; 44: 1222-1230.
5) Warner JR, McIntosh KB. How common are extraribosomal functions of ribosomal proteins? Mol Cell 2009; 34: 3-11.
6) Warner JR. The economics of ribosome biosynthesis in yeast. Trends Biochem Sci 1999; 24: 437-440.
7) Lambertsson A. The minute genes in Drosophila and their molecular functions. Adv Genet 1998; 38: 69-134.
8) Saeboe-Larssen S, Lyamouri M, Merriam J, Oksvold MP, Lambertsson A. Ribosomal protein insufficiency and the minute syndrome in Drosophila: a dose-response relationship. Genetics 1998; 148: 1215-1224.
9) Shenoy N, Kessel R, Bhagat TD, Bhattacharyya S, Yu Y, McMahon C, Verma A. Alterations in the ribosomal machinery in cancer and hematologic disorders. J Hematol Oncol 2012; 5: 32.
10) Naora H, Takai I, Adachi M, Naora H. Altered cellular responses by varying expression of a ribosomal protein gene: sequential coordination of enhancement and suppression of ribosomal protein S3a gene expression induces apoptosis. J Cell Biol 1998; 141: 741-753.
11) Denis MG, Chadeneau C, Lecabellec MT, LeMoullac B, LeMevel B, Meflah K, Lustenberger P. Over-expression of the S13 ribosomal protein in actively growing cells. Int J Cancer 1993; 55: 275-280.
12) Guo X, Shi Y, Gou Y, Li J, Han S, Zhang Y, Huo J, Ning X, Sun L, Chen Y, Sun S, Fan D. Human ribosomal protein S13 promotes gastric cancer growth through down-regulating p27(Kip1). J Cell Mol Med 2011; 15: 296-306.
13) Zhang L, Cilley RE, Chinoy MR. Suppression subtractive hybridization to identify gene expressions in variant and classic small cell lung cancer cell lines. J Surg Res 2000; 93: 108-119.
14) Ganger DR, Hamilton PD, Klos DJ, Jakate S, McChesney L, Fernandez-Pol JA. Differential expression of metallopanstimulin/S27 ribosomal protein in hepatic regeneration and neoplasia. Cancer Detect Prev 2001; 25: 231-236.
15) Vaarala MH, Porvari KS, Kyllonen AP, Mustonen MV, Lukkarinen O, Vihko PT. Several genes encoding ribosomal proteins are over-expressed in prostate-cancer cell lines: confirmation of L7a and L37 over-expression in prostate-cancer tissue samples. Int J Cancer 1998; 78: 27-32.
16) Jimenez L, Becerra A, Landa A. Cloning, expression and partial characterization of a gene encoding the S15a ribosomal protein of Taenia solium. Parasitol Res 2004; 92: 414-420.
17) Shen X, Valencia CA, Szostak JW, Dong B, Liu R. Scanning the human proteome for calmodulin-binding proteins. Proc Natl Acad Sci U S A 2005; 102: 5969-5974.
18) Hannemann J, Velds A, Halfwerk JB, Kreike B, Peterse JL, van de Vijver MJ. Classification of ductal carcinoma in situ by gene expression profiling. Breast Cancer Res 2006; 8: R61.
19) Coleman IM, Kiefer JA, Brown LG, Pitts TE, Nelson PS, Brubaker KD, Vessella RL, Corey E. Inhibition of androgen-independent prostate cancer by estrogenic compounds is associated with

increased expression of immune-related genes. Neoplasia 2006; 8: 862-878.

20) Lian Z, Liu J, Li L, Li X, Tufan NLS, Wu MC, Wang HY, Arbuthnot P, Kew M, Feitelson MA. Human S15a expression is upregulated by hepatitis B virus X protein. Mol Carcinog 2004; 40: 34-46.

21) Xu M, Wang Y, Chen L, Pan B, Chen F, Fang Y, Yu Z, Chen G. Down-regulation of ribosomal protein S15A mRNA with a short hairpin RNA inhibits human hepatic cancer cell growth in vitro. Gene 2014; 536: 84-89.

22) Akiyama N, Matsuo Y, Sai H, Noda M, Kizaka-Kondoh S. Identification of a series of transforming growth factor beta-responsive genes by retrovirus-mediated gene trap screening. Mol Cell Biol 2000; 20: 3266-3273.

23) Zhao X, Shen L, Feng Y, Yu H, Wu X, Chang J, Shen X, QIao J, Wang J. Decreased expression of RPS15A suppresses proliferation of lung cancer cells. Tumour Biol 2015; 36: 6733-6740.

24) Chen J, Wei Y, Feng Q, Ren L, He G, Chang W, Zhu D, Yi T, Lin Q, Tang W, Xu J, Qin X. Ribosomal protein S15A promotes malignant transformation and predicts poor outcome in colorectal cancer through misregulation of p53 signaling pathway. Int J Oncol 2016; 48: 1628-1638.

25) Zheng Z, Cui H, Wang Y, Yao W. Downregulation of RPS15A by miR-29a-3p attenuates cell proliferation in colorectal carcinoma. Biosci Biotechnol Biochem 2019; 83: 2057-2064.

26) Lai MD, Xu J. Ribosomal proteins and colorectal cancer. Curr Genomics 2007; 8: 43-49.

27) Diagnosis, Treatment Guidelines For Colorectal Cancer Working Group C. Chinese Society of Clinical Oncology (CSCO) diagnosis and treatment guidelines for colorectal cancer 2018 (English version). Chin J Cancer Res 2019; 31: 117-134.

28) Zlobec I, Terracciano L, Jass JR, Lugli A. Value of staining intensity in the interpretation of immunohistochemistry for tumor markers in colorectal cancer. Virchows Arch 2007; 451: 763-769.

29) Lois C, Hong EJ, Pease S, Brown EJ, Baltimore D. Germline transmission and tissue-specific expression of transgenes delivered by lentiviral vectors. Science 2002; 295: 868-872.

30) Laemmli UK. Cleavage of structural proteins during the assembly of the head of bacteriophage T4. Nature 1970; 227: 680-685.

31) Liu N, Bi F, Pan Y, Sun L, Xue Y, Shi Y, Yao X, Zheng Y, Fan D. Reversal of the malignant phenotype of gastric cancer cells by inhibition of RhoA expression and activity. Clin Cancer Res 2004; 10: 6239-6247.

32) Wu H, Tschopp J, Lin SC. Smac mimetics and TNFalpha: a dangerous liaison? Cell 2007; 131: 655-658.

33) Darding M, Feltham R, Tenev T, Bianchi K, Benetatos C, Silke J, Meier P. Molecular determinants of Smac mimetic induced degradation of cIAP1 and cIAP2. Cell Death Differ 2011; 18: 1376-1386.

34) Miura K, Karasawa H, Sasaki I. cIAP2 as a therapeutic target in colorectal cancer and other malignancies. Expert Opin Ther Targets 2009; 13: 1333-1345.

35) Neubauer NL, Ward EC, Patel P, Lu Z, Lee I, Blok LJ, Hanifi-Moghaddam P, Schink J, Kim JJ. Progesterone receptor-B induction of BIRC3 protects endometrial cancer cells from AP1-59-mediated apoptosis. Horm Cancer 2011; 2: 170-181.

36) Huang B, Belharazem D, Li L, Kneitz S, Schnabel PA, Rieker RJ, Korner D, Nix W, Schalke B, Muller-Hermelink HK, Ott G, Rosenwald A, Strobel P, Marx A. Anti-apoptotic signature in thymic squamous cell carcinomas--Functional relevance of anti-apoptotic BIRC3 expression in the thymic carcinoma cell line 1889c. Front Oncol 2013; 3: 316.

37) Lan Q, Li S, Lai W, Xu H, Zhang Y, Zeng Y, Lan W, Chu Z. Methyl sartortuoate inhibits colon cancer cell growth by inducing apoptosis and G2/M-phase arrest. Int J Mol Sci 2015; 16: 19401-19418.

38) Zhang C, Yu H, Shen Y, Ni X, Shen S, Das UN. Polyunsaturated fatty acids trigger apoptosis of colon cancer cells through a mitochondrial pathway. Arch Med Sci 2015; 11: 1081-1094.

39) Jagadish N, Parashar D, Gupta N, Agarwal S, Purohit S, Kumar V, Sharma A, Fatima R, Topno AP, Shaha C, Suri A. A-kinase anchor protein 4 (AKAP4) a promising therapeutic target of colorectal cancer. J Exp Clin Cancer Res 2015; 34: 142.

40) Jeggo PA, Lobrich M. Contribution of DNA repair and cell cycle checkpoint arrest to the maintenance of genomic stability. DNA Repair (Amst) 2006; 5: 1192-1198.

41) Warmerdam DO, Brinkman EK, Marteijn JA, Medema RH, Kanaar R, Smits VA. UV-induced G2 checkpoint depends on p38 MAPK and minimal activation of ATR-Chk1 pathway. J Cell Sci 2013; 126: 1923-1930.

42) Mailand N, Falck J, Lukas C, Syljuasen RG, Welcker M, Bartek J, Lukas J. Rapid destruction of human Cdc25A in response to DNA damage. Science 2000; 288: 1425-1429.

43) akai H, Tominaga K, Motoyama N, Minamishima YA, Nagahama H, Tsukiyama T, Ikeda K, Nakayama K, Nakanishi M, Nakayama K. Aberrant cell cycle checkpoint function and early embryonic death in Chk1(-/-) mice. Genes Dev 2000; 14: 1439-1447.

44) Ward IM, Chen J. Histone H2AX is phosphorylated in an ATR-dependent manner in response to replicational stress. J Biol Chem 2001; 276: 47759-47762.

45) Bulavin DV, Higashimoto Y, Popoff IJ, Gaarde WA, Basrur V, Potapova O, Appella E, Fornace AJ Jr. Initiation of a G2/M checkpoint after ultraviolet radiation requires p38 kinase. Nature 2001; 411: 102-107.